

SIMULATION OF MICRO BUNCHING INSTABILITY REGIMES IN THE FLASH BUNCH COMPRESSORS

M. Vogt, T. Limberg, DESY, Hamburg, FRGermany
Donghoon Kuk, The University of Texas at Austin, Austin, TX, USA

Abstract

The bunch compression scheme for the European XFEL [1] will operate in a regime in which, at least without additional energy spread introduced by a laser heater, the micro bunching effect proposed in the literature may severely degrade the performance of the FEL. However, clear, unambiguous signals of the micro bunching effect have not yet been seen neither in simulation nor experiment. In order to establish a parameter regime for experimental verification of micro bunching at the FLASH VUV-FEL at DESY [2], we have simulated and optimized the beam transport with interleaved runs of ASTRA [3] and CSRTrack [4], automatically linked by the start-to-end simulation tool box Gluetrack. We estimated the final current variations starting from shot noise with a quasi-analytic, noise-free gain-model [5].

THE MICRO BUNCHING EFFECT

The micro bunching effect has been numerically studied in the literature before. See, among others, [6, 7]. It is widely believed that *longitudinal space charge* (LSC) is one of the major ingredients to micro bunching in transport channels made from linacs and magnetic chicanes. In this section will discuss micro bunching in purely longitudinal selfconsistent way, thereby ignoring *coherent synchrotron radiation* (CSR). We use Cartesian conjugate coordinates $z := -c\tau$ and $\delta p_z := p_z - p_0$, where c is the vacuum velocity of light, τ is the time-of-flight difference to the reference particle, and p_0 is the reference momentum. All maps M in our model are symplectic so that the phase space density ρ_f after transport through the map is given by the initial density composed with the inverse map $\rho_f = \rho_i \circ M^{-1}$.

In an non-dispersive straight section and in the ultra-relativistic limit, the time-of-flight difference of two arbitrary trajectories is an integral of motion, thus the longitudinal current profile $I(z; s)$ does not depend on s . However, every trajectory may receive different energy changes during the passage of such a section. Thus, the longitudinal phase space density $\rho(z, \delta p_z; s)$ is transformed by a *kick*. Let $\rho_i(z, \delta p_z)$ and $\rho_f(z, \delta p_z)$ be the density before and after passage through such a non-dispersive channel, and $(z, \delta p_z) \mapsto (z, \delta p_z + \Delta[I](z))$ the kick map including a I -dependent LSC term, then

$$\rho_f(z, \delta p_z) = \rho_i(z, \delta p_z - \Delta[I](z)). \quad (1)$$

Since all kicks commute, the momentum change δ (over a

finite distance) has a particularly simple form

$$\Delta[I](z) = f_{\text{cav}}(z) + L \int \langle \mathcal{K}_{\text{lsc}} \rangle(z, z') I(z') dz' \quad (2)$$

where f_{cav} is the integral change through the accelerating structures, $\langle \mathcal{K}_{\text{lsc}} \rangle$ is the kernel for the LSC kick due to a transversely round Gaussian beam [8] with transverse dimensions averaged over s and $L = s_f - s_i$. An *initial* current modulation can generate a *final* energy modulation.

Under the assumption that the magnetic chicanes are short compared to the linacs and fully ignoring synchrotron radiation, in particular CSR, the passage through these chicanes does not change the energy of a particle and thus ρ is transformed by a (generalized) *drift*: $(z, \delta p_z) \mapsto (z + g(\delta p_z), \delta p_z)$ according to

$$\rho_f(z, \delta p_z) = \rho_i(z - g(\delta p_z), \delta p_z) \quad (3)$$

where $g(\delta p_z) := r_{5,6} \delta p_z + O((\delta p_z)^2)$ is the dependence of the path length difference on the momentum deviation. The quantity $r_{5,6}$ for Cartesian longitudinal phase space is related to the more common $R_{5,6}$ for scaled phase space by $r_{5,6} := R_{5,6}/p_0$. If the initial density has a *negative* correlated energy spread $\langle \delta p_z \rangle(z) \approx \delta_0 + hz + O(z^2)$, with $h < 0$, if the uncorrelated energy spread is small $\sigma_E \ll |h|\sigma_z$, and if $r_{5,6} > 0$, then this drift compresses the bunch with compression factor $C := (1 + hR_{5,6})^{-1}$. Typically the energy chirp h is introduced in upstream accelerating modules. The map through the chicane transforms an *initial* energy modulation into a *final* current modulation.

We have seen that the longitudinal space charge in accelerating structures can transform a current modulation into an energy modulation while a subsequent chicane transforms an energy modulation into a current modulation. We consider the composition of the cavity/LSC kick followed by the chicane drift a simplified 2-dimensional (2-d) model of a *bunch compressor stage*. Typical bunch compression schemes used and/or proposed for FEL applications contain one to two (maybe three) stages. Micro bunching means that small initial modulations are amplified during beam transport through successive bunch compressor stages. Various gain mechanisms [6, 7, 5] have been discussed in theory and simulation, but an experimental verification is still missing. For this study we have used start-to-end tracking simulations to find a setup for the FLASH linac with enough gain to see micro bunching seeded by shot noise. The goal was to prepare a *sufficiently long* region of the bunch that supports *high current density* with only *minor variation*. In order to study two stage

micro bunching in a dedicated *region* of the bunch, it is essential to *minimize the mixing* of initially longitudinally separated sub-ensembles through the various stages of the propagation.

FLASH

The injector & bunch compression section of FLASH [2] starts with a RF photo cathode gun capable of producing 5ps long gaussian pulses of 1nC. The laser for the photo cathode is band-width limited and therefore cannot help to seed small wavelength substructures in the bunch. The bunch compression at FLASH in standard SASE op-

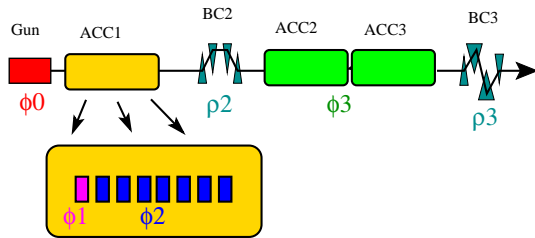


Figure 1: The layout of the 2 stage bunch compression scheme at FLASH.

eration has two stages: First, the bunch is accelerated off crest ($\approx -8^\circ$) in an accelerating module (ACC1) made out of 8 superconducting 9-cell TESLA cavities. Thereby the bunch achieves the energy chirp necessary for bunch compression in the adjacent symmetric 4-dipole chicane (BC2). Second, the bunch is further accelerated (up to -15° off crest) in two more modules (ACC2 & ACC3) and then compressed to its final length in an antisymmetric 6-dipole chicane (BC3). The other parts of FLASH, according to our model, do not potentially contribute much to micro bunching. The two stage compression from gun to BC3 is shown in Fig.1. Due to the large initial bunch length, the bunch strongly samples the non-linearity of the accelerating field in the 1.3GHz cavities, so that the chirp is a function of the position inside the bunch. Thus highest peak currents for SASE operation are typically achieved by over-compression, i.e. inside a small region of the bunch (*spike*) carrying only about 10–20% of the total charge. The spike itself is useless for the micro bunching experiment since it is too short to support modulations of wavelengths observable with the FLASH diagnostics. In order to ameliorate the field non-linearity and achieve high compression rates over a larger portion of the bunch we employed the method of velocity bunching [9] inside the first cavity of ACC1. Finally the 5 parameters to optimize during the simulations are: the RF-phases of the 1-st cavity of ACC1 ϕ_1 , the common phase of the remaining 7 cavities of ACC1 ϕ_2 , the common phase of ACC2 & ACC3 ϕ_3 , and the deflection angles Θ_2 and Θ_3 in BC2 and BC3. The accelerating gradients were chosen for moderate energy gain and adjusted according to operational constraints.

SIMULATIONS

The simulations were performed using the space charge code ASTRA [3] for the gun and the accelerating modules (ACC1-3), the CSR code CSRTrack [4] for the bunch compressor chicanes and the python script Gluetrack to add the kick due to the longitudinal wakefields of the cavities at the end of each ASTRA run, and convert between the different output/input formats. A parallel version of ASTRA using a semi-analytic space charge solver for radially symmetric 3-d charge densities and a serial version of CSRTrack using the projected force model [4] were employed. Since

Table 1: Optimized Set Up

gun	q	1 nC
	ϕ_0	-0.55°
	\mathcal{E}_0^{\max}	44.00 MeV/m
ACC1.Cy ₁	ϕ_1	-83°
	\mathcal{E}_1^{\max}	25.35 MeV/m
ACC1.Cy ₂₋₈	ϕ_2	-2°
	\mathcal{E}_2^{\max}	37.00 MeV/m
	$\langle E_2^{\text{out}} \rangle$	129.3 MeV
BC2	Θ_2	16.49°
	$R_{5,6}$	0.149m
ACC2-3	ϕ_3	-15°
	\mathcal{E}_3^{\max}	30.70 MeV/m
	$\langle E_3^{\text{out}} \rangle$	373.6 MeV
BC3	Θ_3	4.64°
	$R_{5,6}$	0.7329m

a 5-dimensional parameter domain is difficult to scan, a trial-and-error strategy was used. It consists of scanning a parameter, choosing some value as a candidate for the optimum, propagating ensembles generated with the candidate and neighboring values further downstream, evaluating the choice and possibly iterating the choice of the candidate until a decent distribution was achieved at the exit of BC3. The results are summarized in Tab.1 and the longitudinal 2-d projection of the 6-d density at the exit of BC3 is shown in Fig.2. The tracked ensemble contained 200k particles and the density was estimated by projecting the ensemble onto a mesh of 200×200 fixed-size bins and smoothing the result by convolution with a 2-d Gaussian with width of 1.5 bins. The initial ensemble (at the cathode) was sorted by longitudinal position whereby the mixing of longitudinal sub-ensembles could be controlled all along the tracking. As it turned out, a spiked density cannot be completely avoided inside the allowed parameter domain of $(\phi_1, \phi_2, \Theta_2, \phi_3, \Theta_3)$. The goal of high smooth current density over a long range was met best with a $250\mu\text{m}$ long shoulder between 200A and 500A just behind the spike. The (total=summed over sub-ensembles) current density $I(z)$ is shown by the black curve in Fig.3. Additionally the current contributions from 10 longitudinal sub-ensembles (20k each) are indicated by the colored curves. All current densities were computed by filling variable-length bins

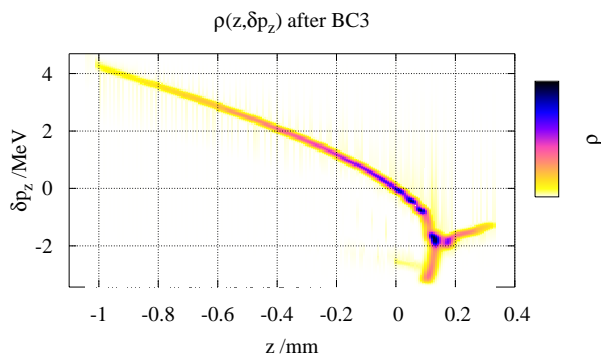


Figure 2: The longitudinal phase space density for the optimized set up at the exit of BC3.

with 500 particles each and Gaussian smoothing. One can

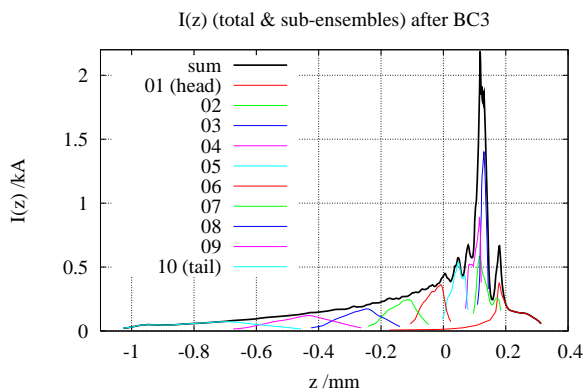


Figure 3: Current profile after BC3 for the optimized set up.

see that sub-ensemble 5,6, and 7 dominate the shoulder population and that their mixing is weak. We do not attempt to ascribe the obvious current modulation in Fig.3 to actual micro bunching. We rather believe it to be an artefact of the small number of macro particles and the longitudinal mesh planes used for the computation of the space charge force. However, we may insert the parameters of our simulation into a quasi-analytic gain model [5] which is based on the 2-d model of micro bunching introduced in the first section and studies the selfconsistent evolution of an infinitely long monochromatic current modulation under the force exerted by itself. This model (for given average transverse size) computes gain curves $G(\lambda_i)$ depending on the initial current I_0 , the $R_{5,6}$'s and the compression factors C . Comparing the average currents for the sub-ensembles constituting the shoulder one obtains compression factors for $C_2 \approx 2.5, 2.1, 2.2$, $C_3 \approx 2.6, 2.3, 2.0$ for BC2 and BC3 and sub-ensemble 5,6,7 respectively. Fig.4 shows the gain after BC2 (blue) and BC3 (red) for sub-ensemble 5 as a function of the initial wavelength. Following [6] the initial current variation is $\sigma_I/I = \sqrt{2ec/I_0\lambda_i}$, which gives $1.5 \cdot 10^{-4}$ to $8 \cdot 10^{-5}$ for λ_i from 50 to 200 μm and $I_0 = 80\text{A}$. It can be concluded that wavelengths in the

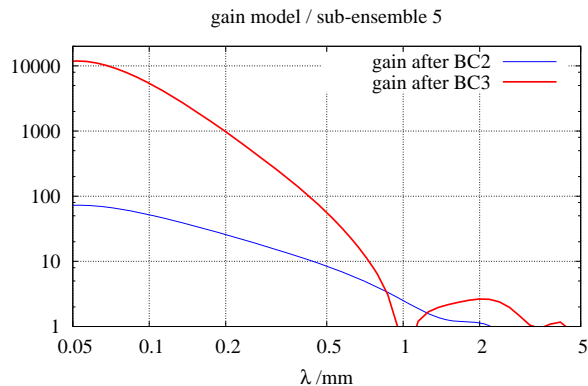


Figure 4: Gain curve for chosen set up according to[5]. The red curve is the combined gain after BC3 while the blue curve is the gain after BC2.

range of 50 to 100 μm (initial) should be highly amplified, and possibly visible, at FLASH with the set up of Tab.1.

REFERENCES

- [1] M. Altarelli *et al.*, "The European X-Ray Free Electron Laser / Technical design report", DESY 2006-097 (2007), also: <http://xfel.desy.de/tdr>
- [2] J. Feldhaus, J. Rossbach, H. Weise, *Physik Journal*, **4/2008** pp.37 (2008).
- [3] K. Flöttmann, "ASTRA / A Space Charge Tracking Algorithm", (2000) http://www.desy.de/~mpyflo/Astra_dokumentation/.
- [4] M. Dohlus, T. Limberg, "CSRTrack Version 1.2 / User's Manual", (2000) <http://www.desy.de/xfel-beam/csrtrack/index.html>.
- [5] M. Dohlus, "Space Charge Instability in XFEL", *talk given at the DESY XFEL Beam Dynamics Seminar* (21.11.2005), http://www.desy.de/xfel-beam/meetings_2005.html. E. Saldin, E. Schneidmiller, M. Yurkov "Longitudinal Space Charge Driven Microbunching Instability in TTF2 Linac" Proceedings of the ICFA Future Light Sources Sub-Panel Mini Workshop on Start-to-End Simulations of X-RAY FELs, Zeuthen, Germany, <http://www.desy.de/s2e/Talks/Monday/>, (August 2003)
- [6] E. L. Saldin, E. A. Schneidmiller, M. V. Yurkov, *Nucl. Inst. Meth. A* **490**, p.1-8 (2002).
- [7] Z. Huang *et al.*, *Phys. Rev. S. T.-A. B.*, **7** 074401 (2004).
- [8] G. Geloni, *et al.*, *DESY 06-222* (2006.)
- [9] B. Beutner *et al.*, "Velocity bunching at the European XFEL", *Proceedings of PAC07, Albuquerque, NM, USA*, p.959-961 (2007).